

†Electronic Supplementary Information (ESI) available: [TEM and electrochemical characterization of monolayer graphene battery]. See DOI: 10.1039/b000000x/

### 1) CVD growth of monolayer graphene.

Chemical vapor deposition (CVD) is an attractive approach to graphene production due to its capability for large area deposition and the lack of intense mechanical and/or chemical treatments. For this method, a wafer with a thin transition metal film plays the role of catalyst. Also, copper foils ranging from 15 μm to 200 μm can be used as a substrate to grow graphene as well. This substrate is placed in a heated furnace and is attached to a gas delivery system, which flows a gaseous carbon feedstock (for example, methane or acetylene) downstream to the metal catalyst foil. It is believed that carbon is then adsorbed and absorbed into the metal surface at high temperatures, where it is then precipitated out in the lowest free energy state (graphene) during the cool down to room temperature. Various growth parameters are varied to determine the optimal fabrication conditions for graphene to grow high quality monolayers or graphene and then a transfer process can be employed to remove the graphene film from the metalized substrate/copper foil onto an oxidized silicon wafer for Raman measurement. The monolayer graphene films used in this experiment were grown using low pressure conditions on top of 25 μm copper foils (from Alfa Aesar) in a cold walled four inch CVD reactor (from Aixtron). The copper foils were annealed at 1000°C under a hydrogen (flow rate of 1000 sccm) and argon (flow rate 150 sccm) atmosphere for 5 minutes prior to the growth. For the graphene growth, methane gas was introduced at a flow rate of 35 sccm for ten minutes at 0.8 mbar pressure conditions. The samples were cooled to room temperature before taking them out from the reactor.

### 2) TEM and electrochemical characterization

As synthesized graphene films were transferred onto Quantifoil (TM) TEM grids with 2 μm holes by a standard transfer procedure [1;2]. The sacrificial polymer layer polymethyl methacrylate (PMMA) was removed via dissolution in acetone. Directly before inserting the samples in the microscope the grids with the film were heated on a hot plate for 5 min at 240°C on air to reduce possible contamination. A Titan G2 60-300 transmission electron microscope (TEM) from FEI, Netherlands equipped with a gun monochromator and imaging Cs corrector was used in order to study the graphene membranes. The operational accelerating voltage used was 80kV and the monochromator was excited to provide an energy distribution of <100 meV in the illuminating electron beam. The Cs value was setup in the range 5-10 μm, and a slightly positive defocus was applied to provide maximum contrast. Under these conditions carbon atoms appear as bright spots.

High resolution TEM provides images of individual atoms as well as the atomic structure of topological defects. The diffraction experiments were performed in Selected Area Electron Diffraction (SAED) mode, where an area from 100nm to 1 μm in size can be selected by an aperture and the diffraction pattern is obtained from this selected area. Spots in the diffraction correspond to the atomic rows and thus indicate the orientation of the crystal lattice. When a few orientations are present in the selected area, a rotation angle between two orientations can be measured as the angular splitting of the reflections. On the other hand, by selecting one of the reflections in the diffraction pattern and building up an image from it (dark field mode) one can image an area of the corresponding lattice. In this manner, different crystal grains can be mapped. Within the suspended monolayer graphene film different grain orientations are observed, Figure S1.

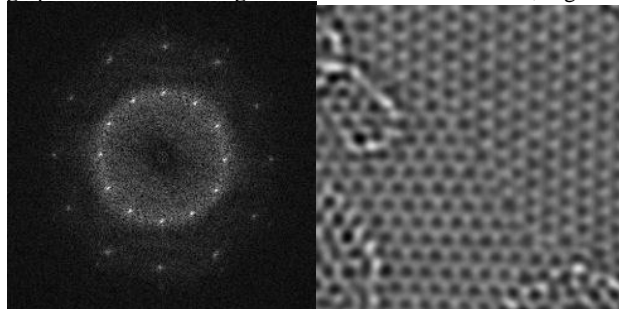


Figure S1 (a) Left corresponding FFT pattern of image (b) Right high resolution TEM image of 30 degree grain boundary between two grains within the monolayer graphene membrane.

The FFT patterns shows two sets of hexagonal patterns related to each of the grain orientations. In this case we observe a 30 degree rotation between the grains as has been previously observed for graphene grown on Cu via CVD [19].

CVD-grown graphene on Cu foil was used as the working electrode and lithium foil as the reference electrode. Such electrodes were assembled into a standard 2032 size coin cell separated by a polymer electrolyte membrane. The polymer electrolyte is wetted by 1 M solution of LiPF<sub>6</sub> in a 1:1 (v/v) mixture of ethylene carbonate and dimethyl carbonate. The open circuit voltage of the graphene cell is about 3V and cyclic voltammetry was carried out between 3V and 0V at a scan rate of 0.1 mV/s. The

electrochemical process of lithium intercalation into the graphene monolayer was studied by cyclic voltammetry and the voltammograms are shown in Figure S2.

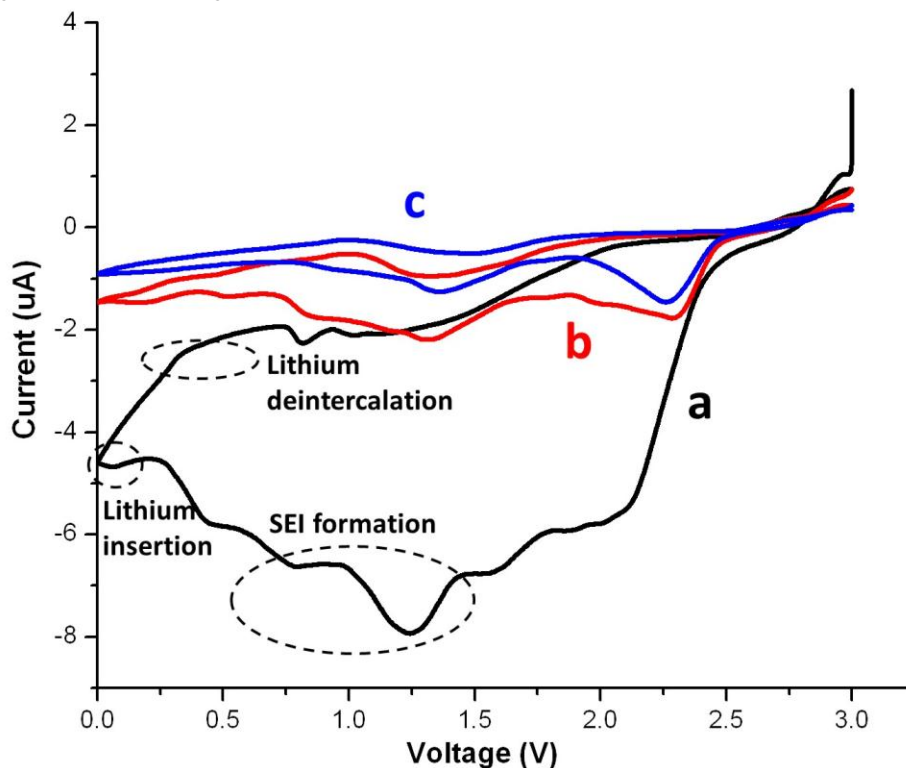


Figure S2 Cyclic voltammograms of the graphene electrode in coin cell with polymer electrolyte wetted by 1 M solution of  $\text{LiPF}_6$  in 1:1 (v/v) mixture of ethylene carbonate and dimethyl carbonate. Li foil is the reference electrode. The scan rate was 0.1 mV/s.

Figure S2 a)-c) shows the voltammograms for the first, second and third cycles for the monolayer graphene on a Cu substrate. The cyclic voltammograms (CVs) display two reduction peaks at 0.7 V and 1.25 V that may correspond to the formation of a solid electrolyte interphase (SEI) layer and irreversible reduction of the electrolyte [3]. The electrode stability may also be affected by the anion groups in the electrolyte which contribute peaks at about 1.25 V [3]. In the second cycle a reduction peak occurs at about 1.33 V, which is slightly higher than the first reduction peak. This may be due to irreversible, structural change and SEI formation [4]. This peak diminishes significantly with cycling but still dominates the electrochemical response at the second cycle. The lithium ion insertion potential is quite low, which is very close to 0 V vs. Li+/Li reference electrode as marked in Figure S2, and in contrast, the potential for lithium ion deintercalation is in the range of 0.2-0.3 V [5]. As is well known, lithiation of graphite is an intercalation process in which lithium is inserted between graphene planes in traditional graphite electrodes. This nature of lithiation process can lead to the voltammetric behavior of the electrode at very low scan rate, such as 0.1 mV/s used in this experiment. Comparing with the lithiation process of conventional graphite, the voltammetric peaks of lithium ion insertion and deintercalation in Figure S2 are smaller, which may be due to that there is only monolayer of graphene in our battery in contrast to the conventional graphite electrode composing stacks of numerous graphene layers. Recent research also find that the interaction of lithium ions with single layer graphene behaves very differently with few-layer graphene, which seem to resemble that of graphite [6 and 7]. The amount of lithium absorbed on defect-free single layer graphene seems to be greatly reduced due to repulsion forces of lithium ions on the graphene layer.

### 3) Calculation of volumetric energy and power density

The volumetric energy and power densities are based on the total volume of monolayer graphene pouch cell battery (whole cell). The area of the pouch cell is 1 cm<sup>2</sup> and total thickness of the cell is 50  $\mu\text{m}$ . The volume of the coin-cell sized pouch cell is  $5 \times 10^{-6}$  L. At current density (I) of 100  $\mu\text{A}/\text{cm}^2$ , the energy capacity (C) is 0.02 mAh/cm<sup>2</sup> and voltage (V) of the cell is 2.5 V.

Thus the power density can be calculated as  $P=I.V$  and energy density can be calculated as  $E=C.V$ . Volumetric power and energy density can thus be calculated with the volume of the pouch cell as 50 W/L and 10 Wh/L. The same calculation applies to the other two current densities (300  $\mu\text{A}/\text{cm}^2$  and 600  $\mu\text{A}/\text{cm}^2$ ) to get three points in the Ragone plot.

### References

S1. X. S. Li, W. W. Cai, J. H. An, S. Kim, J. Nah, D. X. Yang, R. D. Piner, A. Velamakanni, I. Jung, E. Tutuc, S. K. Banerjee, L. Colombo, and R. S. Ruoff, *Science*, 324 (2009) 1312-1314.

- S2. H. J. Park, J. Meyer, S. Roth, and V. Skákalová, *Carbon*, 48 (2010) 1088.  
S3. J. Y. Song, Y. Y. Wang, and C. C. Wan, *J. Power Sources*, 77 (1999) 183.  
S4. M. V. Reddy, B. Pecquenard, P. Vintatier, and A. Levasseur, *Electrochem. Commun.*, 9 (2007) 409.  
S5. A. L. M. Reddy, A. Srivastava, S. R. Gowda, H. Gullapalli, M. Dubey, and P. M. Ajayan, *ACS Nano*, 4 (2011) 6337.  
S6. E. Pollak, B. Geng, K.J. Jeon, I. T. Lucas, T. J. Richardson, F. Wang and R. Kostecki, *Nano Lett.* 10(2010) 3386  
S7. E. Lee and K. A. Persson, *Nano Lett.* 12(2012), 4624